ELSEVIER

Chemical Engineering Journal 72 (1999) 91–95

Chemical Engineering Journal

Vibrocentrifugal fluid pump

Reh-lin Chen*, Steven L. Garrett

Graduate Program in Acoustics, P.O. Box 30, State College, PA 16802, USA

Received 25 March 1998; received in revised form 12 September 1998; accepted 8 October 1998

Abstract

An experimental study of the fluid pumping effect of a clamped-free bar driven at its first resonance frequency is presented. A flexible tube is attached to the bar undergoing oscillatory excitation. The centrifugal force created by the vibration will generate a pressure gradient causing steady, uni-directional fluid flow. This process is extremely attractive for the self-pumping of heat-transport liquids through the heat exchangers in a torsionally resonant toroidal thermoacoustic refrigerator. In that application, a single motor can be used to provide the resonant excitation of the acoustic standing wave within the thermoacoustic refrigerator and eliminates the requirement for two additional motors to pump the hot and cold heat-transport fluids. Measurements are found to agree with simple theoretical predictions.

Keywords: Centrifugal force; Oscillatory excitation; Vibration

1. Introduction

Centrifugal force has been used to create a large variety of pumps with pressure differentials which vary from inches of water (blowers) to more than 10 000 atmospheres (compressors). For example, when water in a cup is stirred vigorously, the water constrained by the curvature of the cup will rise due to centrifugal force [1]. The resulting pressure head depends upon centrifugal acceleration which is directly proportional to the square of the tangential velocity and inversely proportional to the rotational radius. A flexible, corrugated pipe open at both ends can emit sound by holding one end and swinging the free end at some angular velocity. This serves as another demonstration of the use of centrifugal force to provide centrifugal pumping [2,3]. The tones generated by the tube are harmonics of its acoustic resonance frequencies. The emission of sound is determined by periodicity of corrugation and flow velocity which induce turbulence in the tube. It is not surprising in the acoustical demonstration that swinging the tube in an oscillatory manner will also create sound.

A typical centrifugal pump rotates in a single direction. Flow passes through the impeller, picks up rotational energy from it, and develops a pressure head. As the dependence of pressure is quadratic in the rotational velocity, vibratory excitation will also lead to steady, uni-directional fluid flows as in the case of uni-directional fluid pump. Experimental measurements of a vibrocentrifugal pump which is driven by a 'clamped-free' (clamped and driven at one end and free at the other) bar undergoing resonant flexural vibration will be reported. Fluid flow is restricted to a flexible tube attached to, or internal to, the oscillating bar. This process is extremely attractive for the self-pumping of heat-transport liquids through the heat exchangers in a torsionally resonant toroidal thermoacoustic refrigerator [4,5]. In that application, a single motor can be used to provide both the resonant excitation of the acoustic standing wave within the thermoacoustic refrigerator [6,7] and the heat-transport fluid circulation. This eliminates the requirement for two additional motors to pump the hot and cold heat-transport fluids.

2. Theory

The governing equation for thin rod undergoing transverse vibration based on Bernoulli–Euler theory of beams is well known as [8,9]

$$\frac{\partial^2}{\partial x^2}\left(EI\frac{\partial^2 y}{\partial x^2}\right)+\rho A\frac{\partial^2 y}{\partial t^2}=0. \tag{1}$$

For a homogeneous beam with constant cross section, assuming harmonic motion, the above equation can be reduced to

$$\frac{\mathrm{d}^4 y}{\mathrm{d}x^4}-\beta^4 y=0, \tag{2}$$

*Corresponding author.

1385-8947/99/$ – see front matter
PII: S1385-8947(98)00138-7

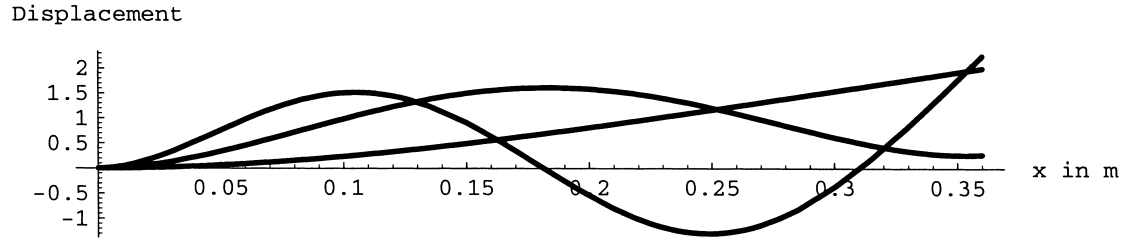

Fig. 1. First three transverse modes of a clamped-free bar.

where $\beta^4=\mu\omega^2/EI$ and μ is linear density of the material. The general solution of Eq. (2) can be expressed as displacement $y(x)=A\cosh\beta x+B\sinh\beta x+C\cos\beta x+D\sin\beta x$. The clamped-free boundary conditions prescribe both displacement and its slope to be zero ($y=0$ and $\partial y/\partial x=0$) at the clamped end. The moment and shear force are both zero ($\partial^2 y/\partial x^2=0$ and $\partial^3 y/\partial x^3=0$) at the free end. This results in the characteristic equation, $\cosh\beta l\cos\beta l+1=0$, which has roots of discrete value. The displacement of nth mode at any given location has the form [10]

$$y_n(x) = (\cosh\beta_n x - \cos\beta_n x) - \frac{\cosh\beta_n l + \cos\beta_n l}{\sinh\beta_n l + \sin\beta_n l}(\sinh\beta_n x - \sin\beta_n x). \quad (3)$$

The natural frequency of the first mode is hence given by $\omega_1 = 3.52/l^2\sqrt{EI/\mu}$.

The aluminum bar used in these experiments is 36 cm long, 6 cm wide, and 4 mm thick. The resonance frequencies of the first three modes of the bar are computed to be f_1=25.7, f_2=160.9, and f_3=450.5 (Hz) (Fig. 1). Here only the first mode is of interest. From the basic centrifugal force formula, we have $\mathrm{d}f(x) = \mathrm{d}m\dot{y}(x)^2/x$, where $\mathrm{d}m$ is the mass within $\mathrm{d}x$ at position x. The amplitude of the transverse velocity at any given location for the first mode is $\omega y_1(x)$. Therefore, $\mathrm{d}p/\mathrm{d}x = \rho\dot{y}_1(x)^2/x$, and the pressure differential between the two ends is

$$\Delta p = \int_0^l \rho\frac{(\omega y_1(x))^2}{x}\mathrm{d}x. \quad (4)$$

To simplify calculation of the centrifugal pressure, the displacement is expressed as a fourth-order polynomial in terms of position along the bar as shown in Fig. 2 where it is compared to the exact solution. Rayleigh's method [11] was used to compute resonance frequency of the first mode. By assuming $y_1(x)=x^4+ax^3+bx^2+cx+d$, coefficients in the polynomial are determined by the four boundary conditions. It follows that $y_1(x)=x^4-4lx^3+6l^2x^2$. The first resonance frequency can then be calculated by equating potential energy with kinetic energy of the transversely vibrating beam. This approximation enables us to easily calculate the centrifugal pressure head, Δp accurately ($\omega_1 = 3.53/l^2\sqrt{EI/\mu}$ from this approximation). The calculated pressure differential at both ends is $0.68(1/2\rho\dot{s}^2)$, where $\dot{s} = \omega y_1(l)$ is tip velocity. Δp has been normalized by kinetic energy density $1/2\rho\dot{s}^2$. The exact solution using Eq. (3) *Mathematica*™ gives $\Delta p = 0.65(1/2\rho\dot{s}^2)$.

The model developed here takes into account dissipation due to several loss mechanisms and incorporates them into the Bernoulli equation. For flow in a pipe, the major losses are shock loss due to abrupt changes in cross-sectional area and viscosity of the fluid. There are also some minor loss mechanisms, for example, roughness and bending. The Bernoulli equation in this application can then be expressed as a sum of pressure heads as

$$h = \frac{v^2}{2} + k\frac{v^2}{2} + f\frac{l}{d}\frac{v^2}{2}, \quad (5)$$

where the first term on the right is due to the energy imparted from transverse oscillation, the second term is shock loss with the constant k determined by the particular experimental geometry, and the third term is frictional loss. The friction factor $f=64/Re_D$ for laminar flow. When flow becomes turbulent, f depends on Re_D and relative roughness e/d [12] and can be found on a Moody chart [13].

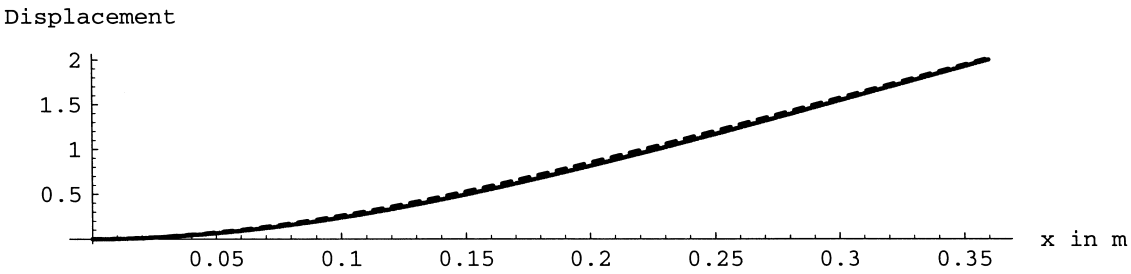

Fig. 2. Displacement distribution along the bar. The solid line represents exact solution and dashed line is an approximation using a fourth-order polynomial.

3. Experiment

In order to test the theoretical predictions, a simple experimental apparatus was designed and instrumented. The core of the vibrocentrifugal pump is an aluminum bar of 36 cm long, 6 cm wide, and 4 mm thick. The bar is clamped and driven at one end by a Brüel and Kjær Type 4813 shaker and free at the other. It is driven at its first resonant mode as shown in Fig. 5. In addition to preliminary calibration of sensors, the experiment has two parts. The first deals with flow rate as a dynamic measurement of flow velocity with respect to pressure head. The second relates bar tip velocity to static pressure built up in the tube due to centrifugal acceleration.

3.1. Calibration of sensors

In order to measure the vibrating velocity of the bar, an accerelerometer is placed at its tip. Four strain gauges, connected as a Wheatstone bridge, were then used to measure displacement in order to cross-calibrate and replace the accelerometer. Static loading measurements were performed to confirm that the bar's behavior conformed with expectation. A linear variable differential transformer (LVDT) was used to measure the end-loaded deflection caused by a known weight W (Fig. 3). Since surface strain at the clamped end is given [14] as $\epsilon=\sigma/E=6Wl/(bt^2E)$ and deflection as $y=-Wl^3/(3EI)$, one can relate end deflection y directly to strain ϵ. The Young's modulus was found to be $7.06\times10^{10}\pm0.8\%$ (Pa) and agrees with typical values for aluminum. The moduli of a material (torsional, longitudinal, and flextural) can also be measured accurately using a resonance technique [15].

3.2. Flow-rate measurement

To check the applicability of Eq. (5) prior to use in the pump, two flexible plastic tubes of 3.25 and 6.5 mm inside diameters and lengths of 72.5 and 95.0 cm, respectively, were connected to a water tank. Fluid flowing out of the tank was measured for known pressure heads. The Reynolds number ranged from ca. 1000 to 4000. Data show that pressure head has a quadratic dependence on flow velocity, while the ratio of flow rate to pressure head varied somewhat from one measurement to another.

The results from typical measurements are shown in Fig. 4 and are fitted using Eq. (6) as

$$\mathrm{d}h = 0.06v + 0.45v^2 \tag{6}$$

where v is the averaged flow velocity based on net mass flow and $\dot{m} = \rho A v\,[\mathrm{kg/s}]$. The flow is found to be only slightly laminar and dominated mostly by turbulence at flow rates typical of our experiment. Difficulties in making accurate comparisons to our theory caused by neglecting turbulence and entrance effects, were overcome by measuring the centrifugically induced static pressure head.

3.3. Static pressure head measurement

A flexible tube was affixed along the top of the aluminum bar with its free end vented to atmosphere and its driven end connected to a water tank, with the water level lower than the free end by 5 to 10 cm. This pumping device was able to draw water out of the tank and discharge at the tip of free end. Tip displacement amplitude for the onset of discharge at the first mode of vibration is around 1 cm. Higher accuracy was obtained using a static approach in which the free end is vented through a capillary tube and the driven end is terminated by an Endevco Model 8530B pressure sensor, as shown in Fig. 5. Calibration was validated by standard laboratory methods. The vibration of the bar generates centrifugal force and induces a pressure differential between the free end (higher pressure) and the driven end (lower pressure). The pressure head is then determined by the pressure sensor output voltage divided by its sensitivity. Water and mercury were used as the fluid media in these

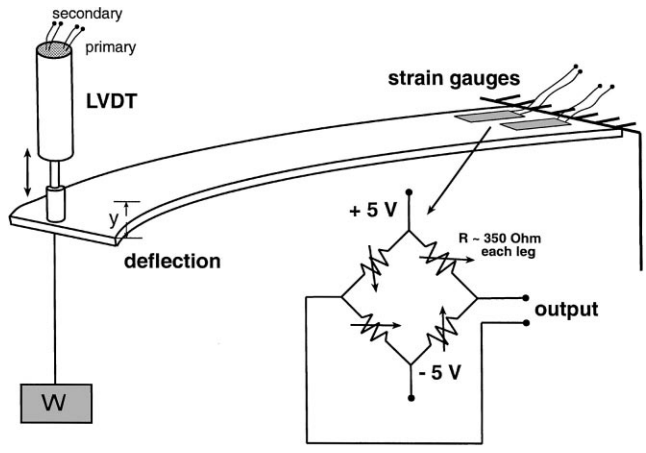

Fig. 3. Experimental setup for measuring deflection due to a known load using LVDT and strain gauges.

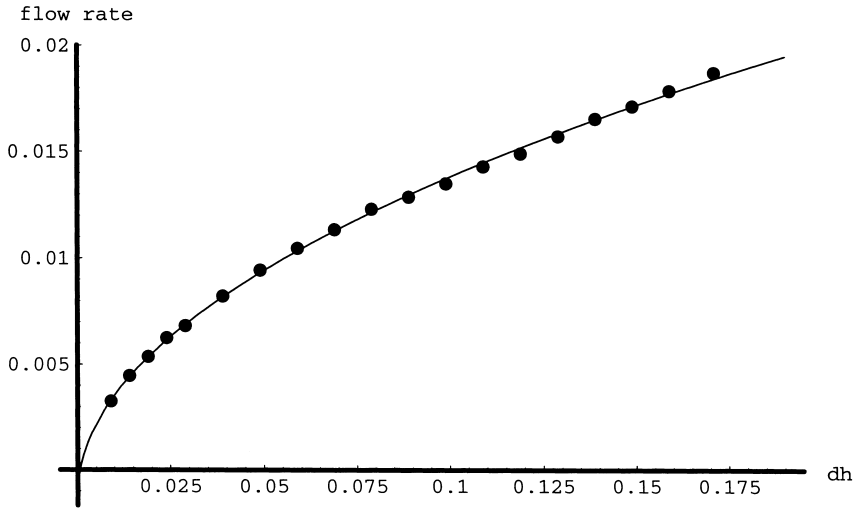

Fig. 4. Flow-rate measurement data with vertical axis plotted in kg/s and horizontal axis as head in m. The points indicate measured data, and the solid line is a quadratic curve fit.

measurements. Figs. 6 and 7 show typical results from this static pressure head measurement.

The driving frequencies were fixed at the first mode which are 21.0 Hz for water and 19.5 Hz for mercury, respectively.

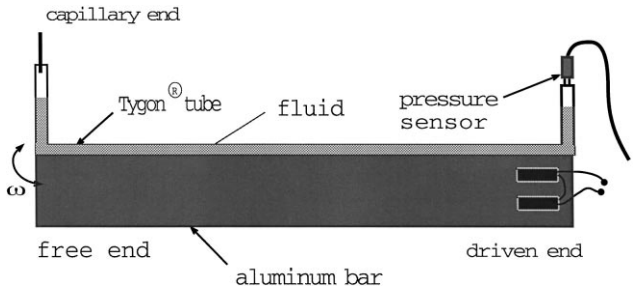

Fig. 5. Setup for measuring pressure differential built up on the right end by vibrocentrifugal force. Two of four bonded resistive strain gauges are shown on the right.

The measured induced pressure differential $\Delta p = k(1/2\rho\dot{s}^2)$ with k varied from 0.47 to 0.57.

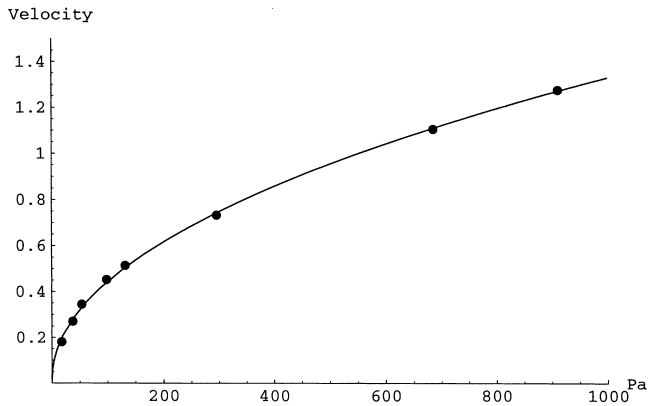

Fig. 6. Tip velocity (m/s) versus induced pressure head for water.

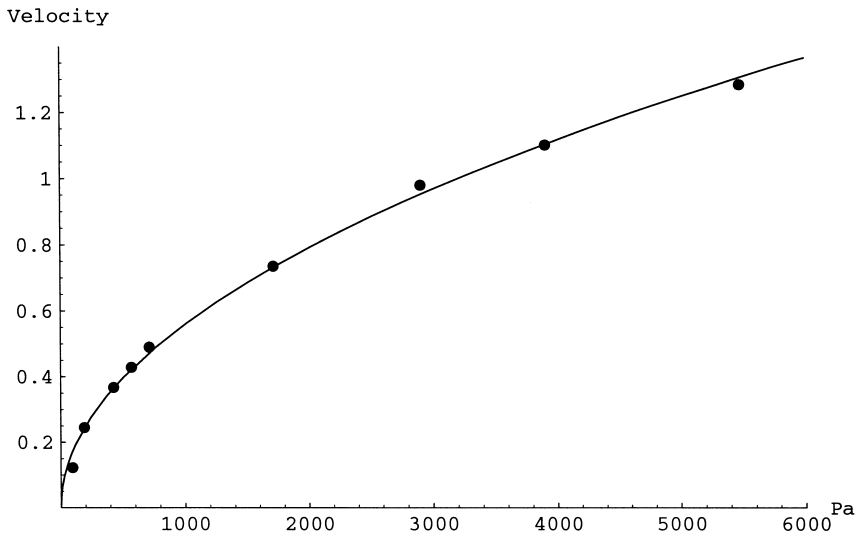

Fig. 7. Tip velocity (m/s) versus induced pressure head for mercury.

4. Results and discussions

Although the flow-rate measurement has a very straightforward setup and dramatic results, these measurements were not well suited to detailed quantitative comparison with the simple theory. It was found in the flow measurement that Reynolds number typically lies in the turbulent and transition regions. The lengths of the flexible tubes typical for implementation were not long enough in order to have fully developed flow. There is also a discontinuity at the connection of the water reservoir to the tube which causes loss, as discussed previously. Nevertheless, the result of pressure head versus velocity is always a parabolic curve with a coefficient determined by a particular experimental geometry.

Since centripetal acceleration is $a_c=(l\theta\omega)^2/l$, induced pressure head depends quadratically on the transverse velocity of the bar and is inversely proportional to its length. A simple approximate theory, valid for small deflections gives the ratio of pressure head to kinetic energy density of 0.68 and agrees with our experimental measurements to an average of 25%. The result is satisfying considering for measurements taken within quasi-turbulent region. We expect that a more robust attachment of the flexible fluid tube to the vibrating bar might improve the agreement between theory and experiment.

Acknowledgements

We would like to thank the Office of Naval Research for sponsoring this work.

Appendix

4.1. Nomenclature

a_c centripetal acceleration (m s^{-2})
A cross-sectional area (m^2)
b width of bar (m)
d diameter of tubes
E Young's modulus (Pa)
g gravitational acceleration $\simeq 9.8$ (m s^{-2})
dh pressure head (m)
I moment of inertia for area (m^4)
l length of a material (m)
$\dot{m}$ mass flow rate (kg s^{-1})
p acoustic pressure (Pa)
Δp pressure drop (Pa)
Re_D Reynolds number
s peak vibration amplitude at aluminum bar tip (m)
$\dot{s}$ peak transverse velocity amplitude at aluminum bar tip (m s^{-1})
t thickness of bar (m)
v averaged fluid velocity (m s^{-1})
W weight of load (N)
y transverse bar deflection (m)
$\dot{y}$ transverse bar velocity (m s^{-1})

4.2. Greek letters

β_n roots of beam equation of mode n
ϵ strain
θ oscillatory angle (rad)
ρ mass density of media (kg m^{-3})
σ stress (Pa)
ω angular frequency (s^{-1})
μ linear mass density (kg m^{-1})

References

[1] H.H. Anderson, Centrifugal Pumps and Allied Machinery, Elsevier Science Publishers Ltd., 4th edn., 1994.
[2] Frank S. Crawford, Singing corrugated pipes, Am. J. Phys. 42 (1974) 278–288.
[3] Louis H. Cadwell, Singing corrugated pipes revisited, Am. J. Phys. 62 (1994) 224–227.
[4] J.W. Osborne, S.L. Garrett, Torsionally Resonant Toroidal Thermoacoustic Refrigerator, 100(4), Pt. 2, (1996) 2816.
[5] Steven L. Garrett, Torsionally Resonant Toroidal Thermoacoustic Refrigerator, U.S. Navy patent case number 77521.
[6] Gregory W. Swift, Thermoacoustic Engines 84 (1988) 1145–1180.
[7] Gregory W. Swift, Thermoacoustic engines and refrigerators, Physics Today 49(7) (1995) 22–28.
[8] Karl F. Graff, Wave Motion in Elastic Solids, Oxford University Press, 1975, chap. 3.
[9] William T. Thomson, Theory of Vibration with Applications, 4th edn., Chapman and Hall, sec. 9.5.
[10] Lawrence E. Kinsler, Austin R. Frey, Allan B. Coppens, James V. Sanders, Fundamentals of Acoustics, 3rd edn., John Wiley and Sons, New York, 1982, p. 73.
[11] J.P. Den Hartog, Mechanical Vibrations, Dover, 1985, chap. 4.5.
[12] Robert W. Fox, Alan T. McDonald, Introduction to Fluid Mechanics, John Wiley and Sons, Inc., 1992, pp. 348–352.
[13] L.F. Moody, Friction factors for pipe flow, Transactions of the ASME 66(8) (1944) 671–684.
[14] Warren C. Young, Roark's Formulas for Stress and Strain, McGraw-Hill, 6th edn., 1989, p. 100.
[15] Steven L. Garrett, Resonant acoustic determination of elastic moduli, J. Acoust. Soc. Am. 88(1) (1990) 210–221.